Journal of Inflammation Research

Dovepress
open access to scientific and medical research

Open Access Full Text Article

ORIGINAL RESEARCH

Moderate Dose Irradiation Induces DNA Damage and Impairments of Barrier and Host Defense in Nasal Epithelial Cells in vitro

Yue-Ying Yang[1,2,*], Jing Liu[2,*], Yi-Tong Liu[3,4], Hsiao-Hui Ong[2], Qian-Min Chen[2,4], Ce-Belle Chen[5], Mark Thong[6], Xinni Xu[6], Sui-Zi Zhou[3,4], Qian-Hui Qiu[3,4], De-Yun Wang[2]

[1]Department of Otolaryngology-Head and Neck Surgery, Zhujiang Hospital, Southern Medical University, Guangzhou, People's Republic of China; [2]Department of Otolaryngology, Infectious Diseases Translational Research Programme, Yong Loo Lin School of Medicine, National University of Singapore, Singapore; [3]Department of Otolaryngology-Head and Neck Surgery, Guangdong Provincial People's Hospital, Guangdong Academy of Medical Sciences, Guangzhou, People's Republic of China; [4]The Second School of Clinical Medicine, Southern Medical University, Guangzhou, People's Republic of China; [5]Centre for Ion Beam Applications, Department of Physics, National University of Singapore, Singapore; [6]Department of Otolaryngology-Head and Neck Surgery, National University Hospital, National University Health System, Singapore

*These authors contributed equally to this work

Correspondence: Qian-Hui Qiu, Department of Otolaryngology-Head and Neck Surgery, Guangdong Provincial People's Hospital, Guangdong Academy of Medical Sciences, No. 106 Zhongshan Road II, Guangzhou, 510080, People's Republic of China, Tel +86 20 83827812, Email qiuqianhui@hotmail.com; De-Yun Wang, Department of Otolaryngology, Infectious Diseases Translational Research Programme, Yong Loo Lin School of Medicine, NUHS Tower Block, 1E Kent Ridge Road, 119228, Singapore, Tel + 65 6772 5373/5370/5371, Fax +65 6775 3820, Email entwdy@nus.edu.sg

Purpose: Radiotherapy (RT) is the mainstay treatment for head and neck cancers. However, chronic and recurrent upper respiratory tract infections and inflammation have been commonly reported in patients post-RT. The underlying mechanisms remain poorly understood.

Method and Materials: We used a well-established model of human nasal epithelial cells (hNECs) that forms a pseudostratified layer in the air-liquid interface (ALI) and exposed it to single or repeated moderate dose γ-irradiation (1Gy). We assessed the DNA damage and evaluated the biological properties of hNECs at different time points post-RT. Further, we explored the host immunity alterations in irradiated hNECs with polyinosinic-polycytidylic acid sodium salt (poly [I:C]) and lipopolysaccharides (LPS).

Results: IR induced DNA double strand breaks (DSBs) and triggered DNA damage response in hNECs. Repeated IR significantly reduced basal cell proliferation with low expression of p63/KRT5 and Ki67, induced cilia loss and inhibited mucus secretion. In addition, IR decreased ZO-1 expression and caused a significant decline in the transepithelial electrical resistance (TEER). Moreover, hyperreactive response against pathogen invasion and disrupted epithelial host defense can be observed in hNECs exposed to repeated IR.

Conclusion: Our study suggests that IR induced prolonged structural and functional impairments of hNECs may contribute to patients post-RT with increased risk of developing chronic and recurrent upper respiratory tract infection and inflammation.

Keywords: human nasal epithelial cells, irradiation, DNA double strand breaks, epithelial barrier, host defense

Introduction

Radiotherapy (RT) is the mainstay of malignant tumors' treatment and has been utilized as the primary treatment in all subsides of head and neck cancer. RT shrink or cure tumors by causing lethal DNA double strand breaks (DSBs) directly or indirectly in targeted tumor cells, resulting in the termination of cell division and proliferation, or even cell necrosis and apoptosis.[1] It affects both tumor cells and adjacent normal cells. After the DSBs' formation, H2AX, one of the histone H2A family members, is phosphorylated into γ-H2AX at the DSB sites.[2,3] Many studies have shown that the γ-H2AX foci appear almost immediately post-irradiation and vanish through a time-dependent manner.[4,5] Since DSB is a critical lesion, failure to restore the chromosome structure can initiate genomic instability and negatively affect cell survival.[4,6]

Some recent studies demonstrated that ionizing radiation (IR) induced injury on epithelial cells. For example, RT causes radiation-induced enteropathy by increasing intestinal permeability and tight junction disruption.[7] The RT

Received: 11 April 2022
Accepted: 16 June 2022
Published: 25 June 2022

generates reactive oxygen species and DNA damage in the oral epithelium and leads to mucositis eventually.[8] IR also damages the integrity of bronchial epithelium in patients with lung cancer post-RT, posing a potential threat of subsequent radiation-induced lung injury.[9]

Nasopharyngeal carcinoma (NPC) is the most common head and neck malignant tumor originating in the nasopharynx. Because of its high sensitivity to IR, especially intensity-modulated RT (IMRT), RT serves as the first choice of NPC management,[10–12] with a five-year overall survival rate of NPC patients post-RT of up to 75%.[13] According to the typical IMRT protocol, the primary tumor site would receive a total radiation dose of 66 to 70Gy in 33 to 35 fractions, 2Gy per fraction, and the frequency is once daily for 5 consecutive days per week for total 6 to 7 weeks.[14] However, throughout the treatment procedure, the nasal mucosa would inadvertently get exposed to approximately 30Gy (equivalent to 1Gy per day),[15] which might induce DSBs in normal epithelial cells and result in subsequent nasal symptoms. It has been reported that the incidence of rhinosinusitis in NPC patients who received IMRT is up to 73.5%.[16] In our previous study, we observed long-term epithelium barrier defects and aberrant morphological changes in the inferior turbinate of NPC patients post-RT,[15] and the biopsies collected from patients suffered from radiation-induced chronic rhinosinusitis that manifested a more severe epithelial remodeling.[17] Furthermore, several studies also found that the mucociliary clearance remarkably decreased in patients who endured RT.[18,19] Those findings indicated that IR induced damage of airway epithelium and increased the susceptibility of these patients to respiratory tract infections and inflammation.

The human nasal epithelium is composed of basal cells, secretory cells, and ciliated or nonciliated columnar cells with distinct proportions.[20] Under homeostatic circumstance, the epithelium is not only capable for self-renewal,[21] but also contributes to physiological barrier[22] and host defense.[23] However, whether exposure to peripheral doses of below treatment levels radiation-induced would induce DNA damage in nasal epithelial cells leading to long-term defects, remains poorly understood. We have been successful in isolating adult human nasal epithelial stem/progenitor cells (hNESPCs) from nasal biopsies.[24,25] The hNESPCs are able to differentiate into pseudostratified nasal epithelium in ALI culture, which is composed of both ciliated columnar cells and goblet cells on top, while maintaining an immature phenotype. Therefore, this in vitro epithelium model allows us to study the long-term effect of irradiation on the mechanical barrier and the innate immune response of the nasal epithelium in response to single and repeated exposure (5 days) to moderate dose (1 Gy) of irradiation. This experiment setup aimed at mimicking a post-irradiation epithelium conditions in vivo and investigating the long-term effect of IR on normal nasal epithelial cells. Understanding the molecular events driving the normal tissue injury is important in developing preventions and treatment of IR-induced toxicities.

Materials and Methods

hNECs Culture, Irradiation, and Treatment

The hNECs were differentiated from hNESPCs isolated from inferior turbinate of healthy subjects (n = 9) who underwent septal plastic surgery at the National University Hospital of Singapore. None of them had upper respiratory tract infections or any type of rhinosinusitis. They were not taking any forms of glucocorticoids, anti-inflammatory agents, or antibiotics within 3 months before the surgery. Approval to conduct this study was obtained from the National Healthcare Group Domain-Specific Board of Singapore (DSRB code D/11/228). The hNESPCs were transferred to an ALI system to form a pseudostratified layer within 4 weeks. Methods for culturing hNECs were described in the previous paper.[24]

On ALI day 1, cells were exposed to 1Gy irradiation in a ^{60}Co source irradiator (Gamma Chamber 4000A, Board of Radiation & Isotope Technology, India) using a dose rate of 0.56 Gy/min. The cells for irradiation were divided into two different groups, the IR1 group was exposed to single time irradiation on ALI day 1, the IR5 group received a repeated exposure from ALI day 1 to day 5. In the meantime, the control cells experienced mock irradiation by being placed outside the room of the irradiator. After finishing the irradiation, both irradiated and control cells continued to culture until they were fully differentiated and harvested on ALI day 14 and ALI day 28.

For the stimulating experiments, the medium containing 25 μg/mL Poly(I:C) or 10 μg/mL LPS was added to the control and IR5 groups on the ALI day 28. After 24 hours of stimulation, we harvested the cells for further analysis.

Cytospin Preparation

Dissociated hNECs with 1×Trypsin/EDTA solution (Gibco, Carlsbad, CA, United States) and then fixed in 4% paraformaldehyde at room temperature for 10 min followed by PBS wash. Cytospin ($1–2\times10^4$cells/slide) was prepared at 500 rpm for 5 min by using Shandon Cytospin 4 Cytocentrifuge (Thermo Fisher Scientific, Pittsburgh PA, United States).

Immunofluorescent (IF) Staining

Cytospin samples and transwell membranes of ALI culture were used to perform IF staining. Briefly, samples were fixed and permeabilized with 0.1% Triton-X, then blocked with 10% goat serum and subsequently incubated with a primary antibody (Table 1) overnight at 4°C. The next day, samples were washed with 1× PBS three times, followed by 60 min incubation of Alexa Fluor 488- or Alexa Fluor 594-conjugated secondary antibodies (1:500, Invitrogen, A11029 & A21145 & A10037) in the dark at room temperature. Mounting medium with 4′6-diamidino-2-phenylindole (DAPI) (Invitrogen, Carlsbad, CA) was used to stain cell nucleus.

Foci Counting Method

Immunofluorescent images were captured by fluorescent microscope (Olympus IX51, Tokyo, Japan) at 400× magnification. Five individual views from each IR or time-matched control membrane were assessed. The foci were counted manually in at least 500 cells. The foci per nucleus were calculated by the following formula: total foci per view/total DAPI per view. For the foci over 30 pixels, we used FIJI software to distinguish and manually exclude the selected point not overlapped with DAPI.

Western Blotting

The preparation of the cell lysates, SDS-PAGE and Western blot analysis were performed according to standard protocols. The PVDF membrane was incubated respectively with primary antibody (Table 1) overnight at 4°C on shaker. After incubating with HRP-linked secondary antibody (1:2000, Invitrogen, 31,430 and 32,460) for 1 hour at room temperature, the protein bands were detected using the iBright 1500 Image system (Thermo Fisher Scientific, Pittsburgh PA, United States) and assessed the ratio of target protein against house-keeping protein.

RNA Isolation and Quantitative Real-Time Polymerase Chain Reaction (RT-qPCR)

Total RNA was extracted from hNECs using the mirVana miRNA Isolation Kit (Life Technologies, Grand Island, NY, United States). Complementary DNA was synthesized in a 20 μL reaction volume from 1 μg total RNA. Then, relative gene expression was detected using SYBR green gene expression assay on CFX Connect Real-Time PCR Detection System (Bio-Rad, Hercules, California, United States) and was normalized to $2^{-\Delta\Delta Ct}$ with ribosomal protein L13a (RPL13A) as a housekeeping gene. Details of primer sequences could be found in Table 2.

Table 1 Antibodies and Dilutions Used for IF or Western Blot

Antibody	Host	Type	Dilution		Catalog	Company
			IF	WB		
γ-H2AX	Ms	Monoclonal	1:300	1:1000	JBW301	Millipore
ZO-1	Rb	Polyclonal	1:400	1:1000	HPA001636	Sigma
FOXJ1	Rb	Polyclonal	1:300	1:1000	HPA005714	Sigma
MUC5AC	Rb	Polyclonal	1:500		sc-20118	Santa Cruz
MUC5AC	Rb	Monoclonal		1:10,000	ab198294	Abcam
GAPDH	Ms	Monoclonal		1:10,000	ab8245	Abcam
Ki67	Rb	Monoclonal	1:400		ab16667	Abcam
KRT5	Rb	Monoclonal	1:600		ab52635	Abcam
p63	Ms	Monoclonal	1:50		ab735	Abcam
Ace-α-tubulin	Ms	Monoclonal	1:1000		ab24610	Abcam

Table 2 Primers Used for RT-qPCR

Target Gene	Sequence (Forward, 5'-3')	Sequence (Reverse, 5'-3')
RPL13A	GTCTGAAGCCTACAAGAAAG	TGTCAATTTTCTTCTCCACG
FOXJ1	GTGAAGCCTCCCTACTC	AATTCTGCCAGGTGGG
MUC5AC	AATGGTGGAGATTTTGACAC	TTCTTGTTCAGGCAAATCAG
ZO-1	TTGTCTTCAAAAACTCCCAC	GACTCACAGGAATAGCTTTAG
Ki67	GACAGAGGTTCCTAAGAGAG	AACAATCAGATTTGCTTCCG
p63	CAGCCTATATGTTCAGTTCAG	CAGTCCATGCTAATCTCAATC
KRT5	TGGAAGACTTCAAGAACAAG	ATGTAGGCAGCATCTACATC
DNAI1	TCAGTGGGAGATCTATGATG	ACTCCATAGATATCAGCTTC
DNAI2	GAAGTGGAAGAAGACTTAGC	CTTTCTGTTCCTGATTTGTAGG
DNAH2	AGATCCAGAGATACAACACAC	ATTGAAAATCTCTTCCAGGC
DNAH3	AATACTAGCGGGAAAATTGC	CACTTHTTGAGAAGAGTCTG
DNAH5	ACTGATGCAACTAATGAAGC	AGTGTAGGAATAGCATCCATC
DNAH6	CATGGGTCAAAGACCTTATC	GTTCCTGTTAGAAATCCTTGAG
DNAH12	AGGTCCTTTACCTGAATCTC	GTTGTATAACCAAGGTCCAG
RSPH1	GGAAAGAGGAGAAGAGGAAG	AATTCAGTGATTTGGGTAGC
RSPH4A	TTTGACACCAATCTCTGAAG	TTGTGGAATGAGATTTGAGG
RSPH9	GAATATGAACACACTGAGCTG	CTTGATCTGGACCACTATTTC
TLR3	AGATTCAAGGTACATCATGC	CAATTTATGACGAAAGGCAC
CXCL10	AAAGCAGTTAGCAAGGAAAG	TCATTGGTCACCTTTTAGTG
IFNB1	ATTCTAACTGCAACCTTTCG	GTTGTAGCTCATGGAAAGAG
IL28A	ACATAGCCCAGTTCAAGTC	GACTCTTCTAAGGCATCTTTG
RSAD2	GCTCTAAGAGAAGCAGAAAG	CATCTTCTGGTTAGATTCAGG
TLR4	GATTTATCCAGGTGTGAAATCC	TATTAAGGTAGAGAGGTGGC
CCL2	AGACTAACCCAGAAACATCC	ATTGATTGCATCTGGCTG
IL-6	GCAGAAAAAGGCAAAGAATC	CTACATTTGCCGAAGAGC
IL-8	GTTTTTGAAGAGGGCTGAG	TTTGCTTGAAGTTTCACTGG
IL-17A	GTATGAGAAAAGTTCAGCCC	TGGTTACGATGTGAAACTTG

Transepithelial Electrical Resistance (TEER)

TEER was measured for control and IR cells using an epithelial volt/ohm meter (EVOM2) (World Precision Instruments, Sarasota, FL, United States) at ALI day 28; the value of TEER was calculated by subtracting the blank well measurement and presented as $\Omega \cdot cm^2$.

Ciliary Beat Frequency Assessment (CBF)

Before measurement, cells were washed with 1×dPBS at 37°C. CBF was then analyzed at room temperature using the Sisson-Ammons Video Analysis system (SAVA, Omaha, NE, United States) with an inverted microscope (Olympus, Tokyo, Japan) at a magnification of 200×. Actively beating ciliated cells from each experiment in ALI culture were assessed, respectively, before harvesting. For all experiments, the predominant frequency of a small group of cilia from each sample was viewed and taken in at least three separate fields every 30s for up to 3 min. At the same time, they were maintained at a constant temperature (23 ± 0.5°C). All frequencies from each sample are expressed as the mean from each field over 3 min.

Statistical Analysis

Statistical analysis was performed using GraphPad Prism 8 software (GraphPad Software Inc., San Diego, CA, United States). Mann–Whitney two-tailed test was used to analyze the differences among control and treatment groups. $P < 0.05$ was considered statistically significant.

Results

IR Induces Cell DNA Double Strands to Break and Repair Within 24h Post-Irradiation

In our study, we chose a moderate dose gamma IR on hNECs corresponding to the expected peripheral dose during RT.[15] Our pilot studies carried out at higher doses of 2Gy demonstrated a decrease in cell viability compared to 1Gy (Figure S1A). Therefore, we used 1Gy as the subsequent treatment dose in the following experiments at varying time points on the 0–24h scale for both single (IR1) and repeated (IR5) irradiation. We first assessed the radiation-induced DNA damage and repair kinetics of DSBs by using γ-H2AX immunofluorescence (IF) assay. DSBs' detection and foci quantification were performed at 1h, 3h, 6h, and 24h (Figure 1A). According to the IF result, we observed that γ-H2AX foci formation peaked at 1h post-irradiation and gradually reduced to baseline by 24h post-irradiation for both IR1 and IR5 groups (Figure 1B). Compared to the time-matched control cells, the IR groups displayed a robust increase in the number of γ-H2AX foci per nucleus (Figure 1C and D), indicating that IR caused hNECs DNA damage. We also performed Western blot to detect the γ-H2AX protein level (Figure S1B). We observed elevated γ-H2AX signal in both IR1 and IR5 groups at 1h post-IR (Figure S1C and D). Although it did not show a time-dependent decrease compared to the time-matched control cells, the result still demonstrated that IR induced DSBs and triggered DNA damage response in hNECs.

Moreover, we noticed that the foci varied from one another in size. Thus, we further investigated the foci number over 30 pixels. In both IR1 and IR5 groups, the number of foci >30 pixels decreased in a time-dependent manner. The number of >30 pixels foci reached a higher level at 1h post-IR in the IR1 group and ultimately went down to baseline level at 24h post-IR. However, the number of >30 pixels foci at 24h post-IR in the IR5 group remained detectable (Figure 1E and F). These findings indicated a reduced repair efficiency in the IR5 group.

IR Disrupts the Proliferation of hNECs

In order to investigate the influence of moderate dose irradiation on hNECs proliferation and differentiation, both irradiated and control cells were continually cultured until fully differentiated (Figure 2A). According to the cytospin IF staining result, the ratio of p63 and keratin 5 (KRT5) double-positive cells, representing basal cells, significantly decreased in the IR5 group in comparison to the control on ALI day 28 but not on ALI day 14. We found no significant reduction in the ratio of basal cells between the IR1 group and the control group on both ALI day 14 and day 28 (Figure 2B and C). The ratio of Ki67 positive cells (proliferation marker) also significantly decreased in the IR5 group in comparison to the control on ALI day 28 but not on ALI day 14. The ratio of Ki67 positive cells in the IR1 group did not show a significant reduction in comparison to the control on both ALI day 14 and day 28 (Figure 2D and E). In contrast with the protein level, the mRNA levels of Ki67, p63, and KRT5 showed an increasing trend on both day 14 and day 28 in comparison to the control (Figure S2A–C), which indicated a compensatory transcription of damaged proliferation.

Collectively, a reduced ratio of proliferative basal cells indicated that repeated exposure to moderate dose irradiation might affect the differentiative ability of hNECs function.

IR Leads to an Altered Differentiation of Goblet Cells and Ciliated Cells in hNECs

The normal epithelium can differentiate into ciliated and goblet cells under ALI culture conditions. We investigated whether IR affected the differentiation of hNECs. IF staining was performed for phenotyping goblet cells and ciliated cells (Figure 3A). From IF, we could observe a significant reduction in the positive area of goblet cell marker MUC5AC in both IR1 and IR5 groups (Figure 3B). MUC5AC was significantly elevated in mRNA expression at day 28 in the IR5 group (Figure 3C). However, in contrast to the increased mRNA level, the Western blot results revealed a down-regulation of MUC5AC in both IR1 and IR5 groups (Figure 3D). The IF staining result showed a significant reduction in the cilia area in the IR5 group compared with the untreated control group, while the IR1 group maintained a similar cilia density as the control group (Figure 3E). Then, we further investigated the ciliated cell marker FOXJ1. The mRNA level of FOXJ1, however, increased significantly in the IR5 group (Figure 3F), but we found a significant reduction in the protein level in the IR5 group (Figure 3G).

In our previous study, we found that abnormal ciliogenesis is associated with ultrastructural abnormalities in ciliated cells.[26] Thus, we further investigated the expression of motile cilia assembly markers, such as the outer dynein arm genes

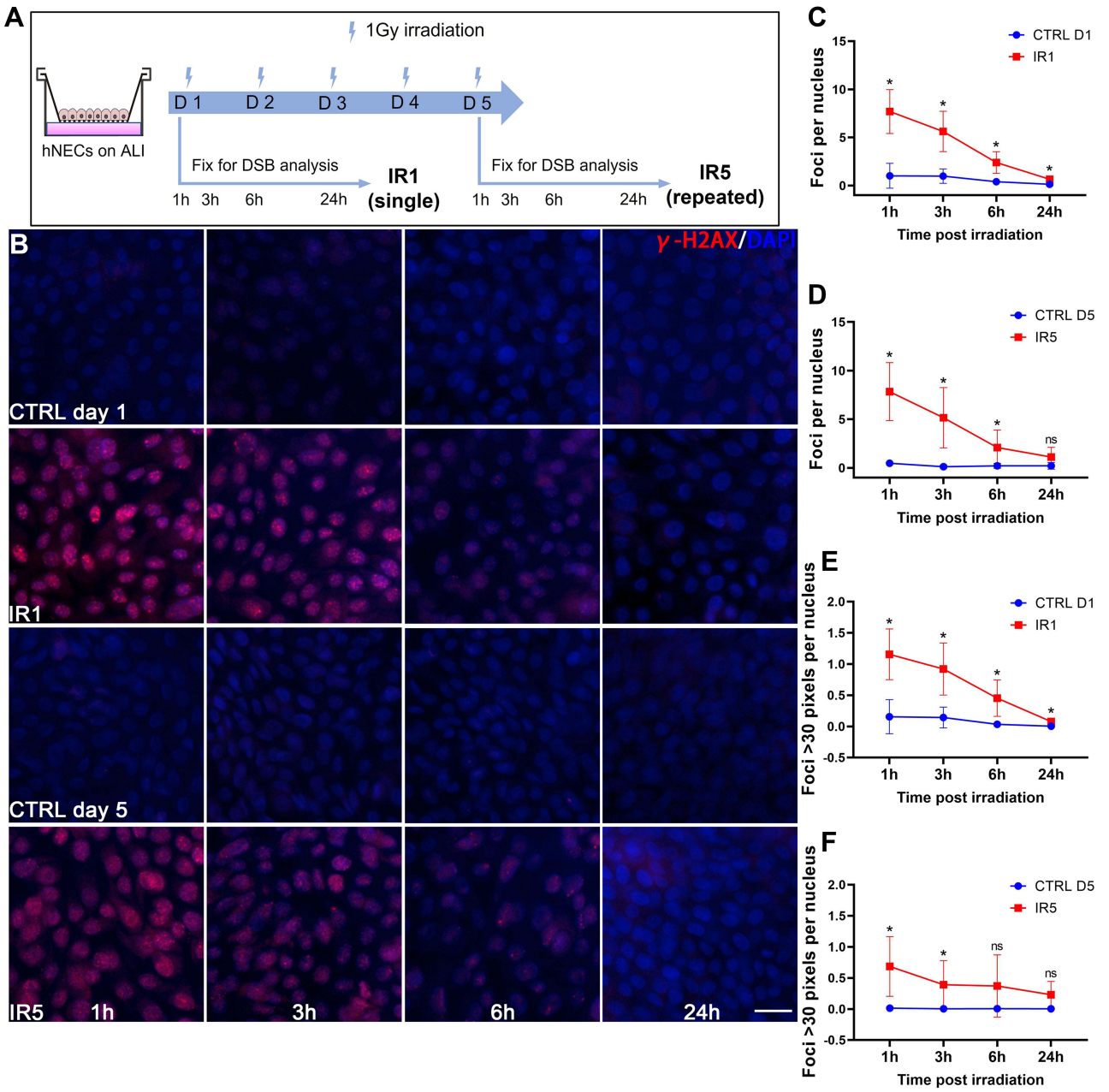

Figure 1 Decreasing γ-H2AX foci in irradiated cells over time. (**A**) Schematic for ALI culture hNECs irradiation timeline. (**B**) IF staining images showed γ-H2AX foci (red) within the nucleus (blue) decreased in a time-dependent manner, (×400 magnification, scale bar = 20μm). (**C**–**D**) Foci per nucleus were counted manually (counted at ×400 magnification, 5 different views of same donor at each time point). (**E**–**F**) The number of foci > 30 pixels per nucleus (counted at ×400 magnification, 5 different views of same donor). Error bars represent mean with standard deviation from 4 different donors. P > 0.05 is presented as "ns"; P < 0.05 is presented as "*". IR1: hNECs that exposed to single irradiation; IR5: hNECs that exposed to repeated irradiation; CTRL: the untreated hNECs.

and radial spoke head genes. We found that the outer dynein arm heavy chain genes DNAH5, DNAH6, DNAH12 decreased significantly in both IR1 and IR5 groups. The outer dynein arm heavy chain genes DNAH2, DNAH3, and intermediate chain genes DNAI1, DNAI2 were also significantly downregulated by irradiation in the IR1 group (Figure 4A–G). However, the mRNA level of radial spoke head protein showed no significant difference between the IR and the control group (Figure S3A–C). The irradiation resulted in a downregulation in the outer dynein arm genes, and the ciliary beating frequency slightly decreased in the IR1 and the IR5 groups compared to the control group, which indicated that the remaining cilia in the IR cells may have defective motility (Figure 4H).

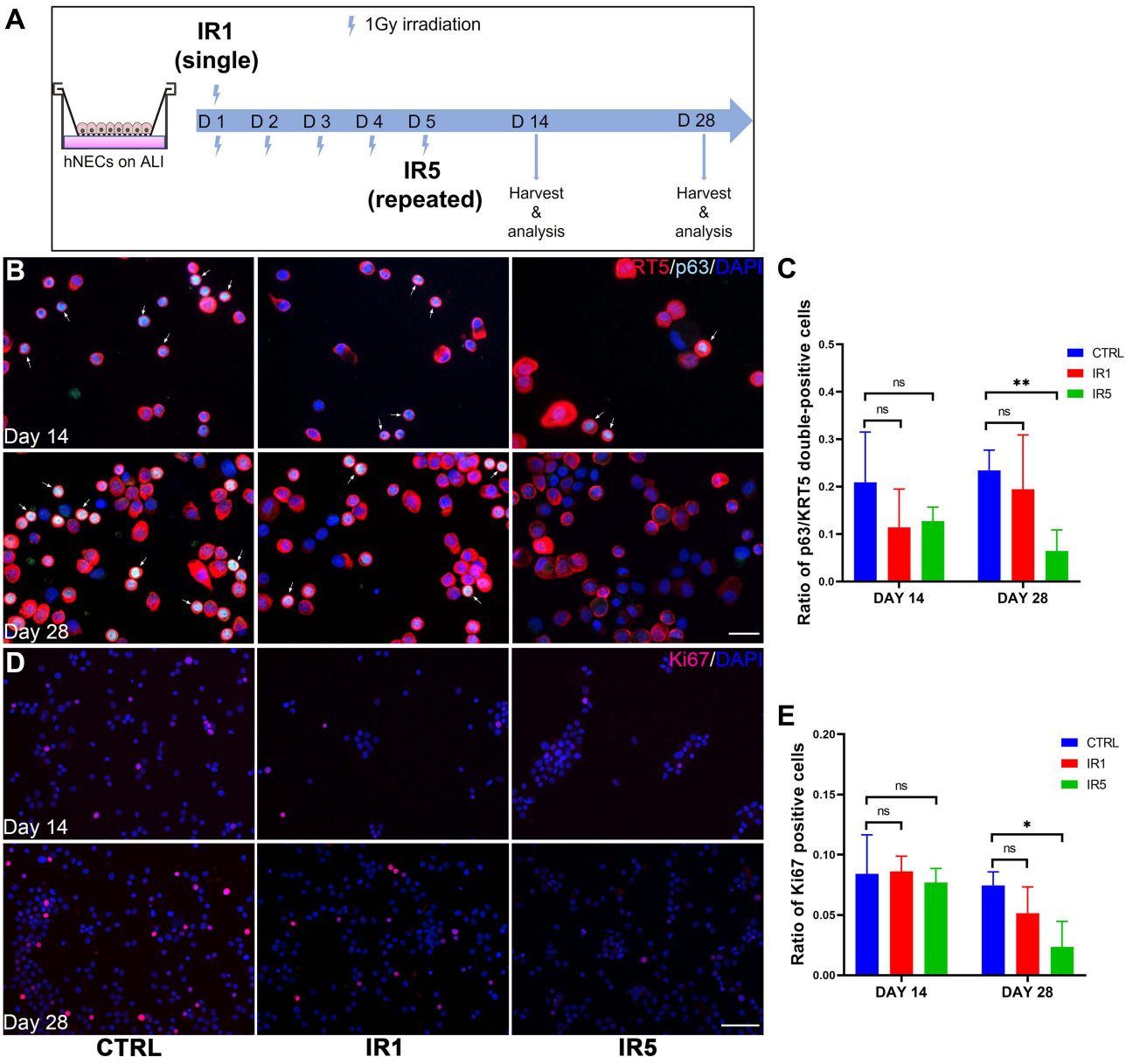

Figure 2 Effect of irradiation on hNECs proliferation. (**A**) Schematic for post-IR hNECs culture and harvest timeline. (**B**) Representative IF staining images show decreased p63 and KRT5 double-positive cells (white arrow pointed cells, ×400 magnification, scale bar = 20μm) in IR5 group on ALI day 28. (**C**) Representative IF staining images show decreased Ki67 positive cells (×200 magnification, scale bar = 50μm) in IR5 group on ALI day 28. (**D**–**E**) The ratio of p63 and KRT5 double-positive cells and Ki67 positive cells decreased significantly in IR5 group in comparison to the control on ALI day 28 but not on day 14, while the IR1 group did not show a significant reduction in comparison to the control on both ALI day 14 and day 28. (The number of positive cells was counted at ×200 magnification, 5 views per treatment; day 14, n = 3; day 28, n = 6). Error bars represent median with interquartile range. P > 0.05 is presented as "ns"; P < 0.05 is presented as "*" P < 0.01 is presented as "**". IR1: hNECs that exposed to single irradiation; IR5: hNECs that exposed to repeated irradiation; CTRL: The untreated hNECs.

IR Induces Epithelial Cell Barrier Function Defects

Since IR altered differentiation of hNECs suggests disruption of epithelial integrity and may impair barrier function, we next compared the mRNA level and morphological pattern of tight junction marker ZO-1 in different groups. As shown, IR5 strongly affected cell morphology as observed from ZO-1 staining displaying an irregular pattern, which was less continuous along the cell boundary compared with the control and IR1 groups (Figure 5A). However, the mRNA level of ZO-1 had no significant difference between the control and IR groups (Figure 5B). Immunoblot data showed a decreased level of ZO-1 protein in the IR5 group (Figure 5C). As expected, the transepithelial electrical resistance measurement revealed that the IR5

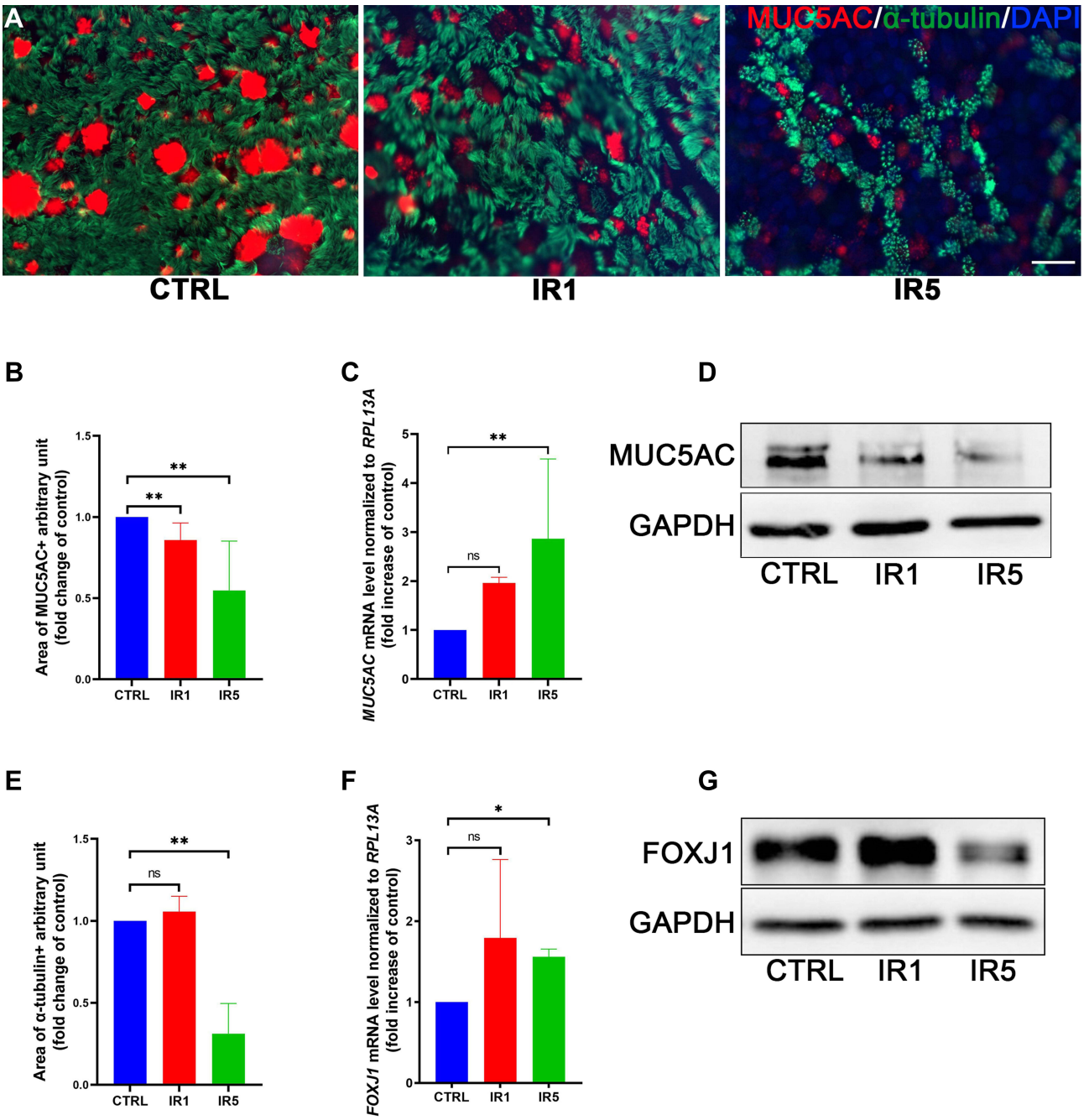

Figure 3 Effect of irradiation on hNECs differentiation. (**A**–**C**) Representative transwell IF images of goblet cells (red, MUC5AC) and ciliated cells (green, α-tubulin) double staining at ALI day 28 (×400 magnification, scale bar = 20 μm). The IR5 group shows a significant decrease in the ratio of ciliated cells (α-Tubulin+) and goblet cells (MUC5AC+) area (n = 5). (**D**) The MUC5AC mRNA level increased significantly in the IR5 group on ALI day 28 (n = 9). (**E**) The FOXJ1 mRNA level increased significantly in the IR5 group on ALI day 28 (n = 9). (**F**–**G**) Western blot results confirmed a significant decrease in the protein level of MUC5AC and FOXJ1 in the IR5 group. Error bars represent median with interquartile range. P > 0.05 is presented as "ns"; P < 0.05 is presented as "*"; P < 0.01 is presented as "**". IR1: hNECs that exposed to single irradiation; IR5: hNECs that exposed to repeated irradiation; CTRL: The untreated hNECs.

group reduced significantly in TEER values in comparison to the control on both ALI day 14 and day 28, while the TEER values of the IR1 group showed no difference on both ALI day 14 and day 28 in comparison to the control (Figure 5D).

Taken together, these results indicate that repeated exposure to moderate dose irradiation plays a role in damaging the epithelial barrier integrity.

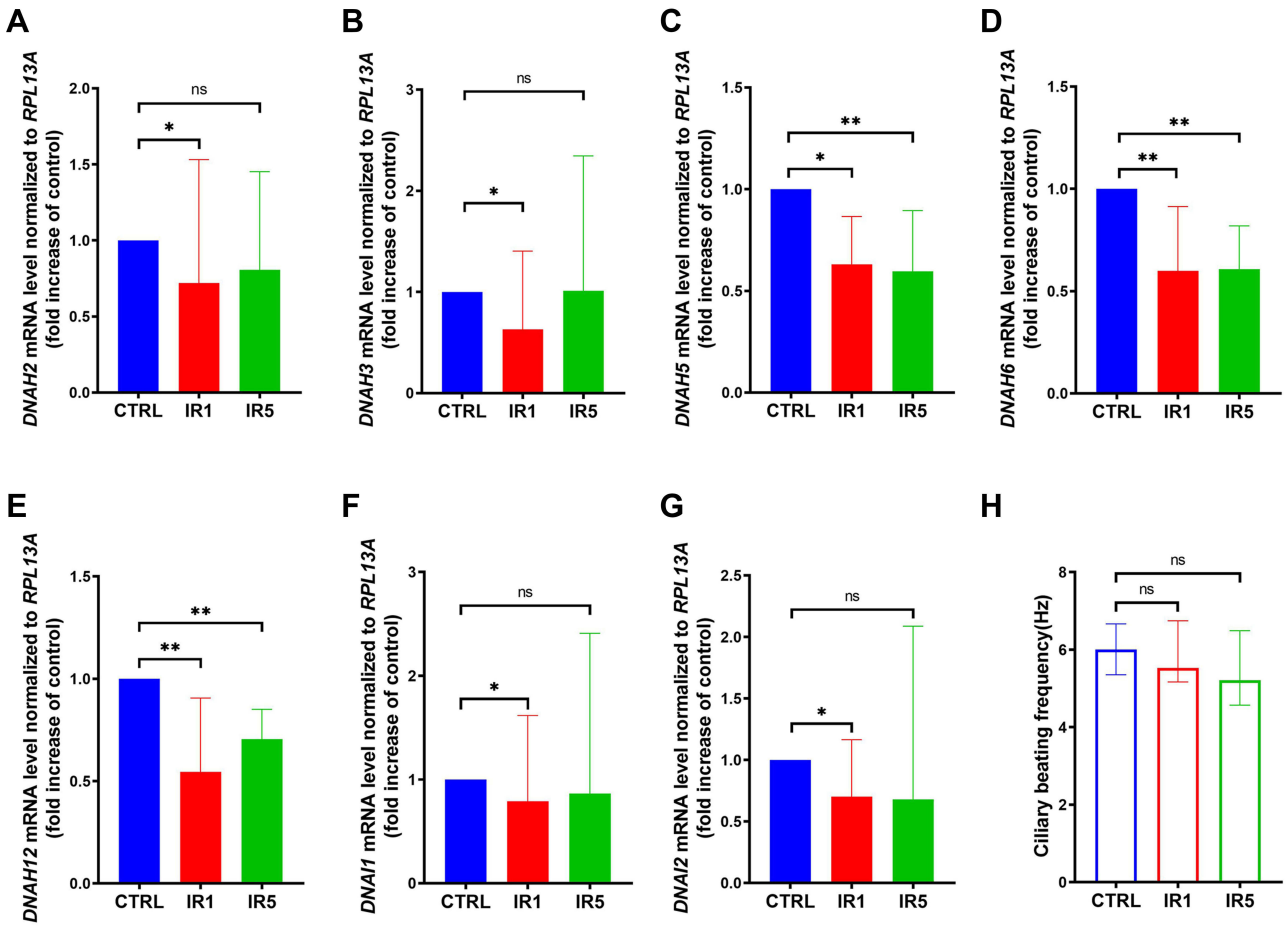

Figure 4 Ultrastructural alteration of ciliated cells exposed to IR. (**A**–**G**) mRNA level of outer dynein arm heavy chain and intermediate chain markers DNAH5, DNAH6, DNAH12 are decreased significantly in both IR1 and IR5 groups, while DNAH2, DNAH3, DHAI1, DNAI2 only significantly decreased in the IR1 group (n = 9). (**H**) Ciliary beating frequency (CBF) was auto analyzed using the SAVA system on ALI day 28, a decreasing trend of CBF was detected in the IR1 and IR5 groups (n = 8). Error bars represent median with interquartile range. P > 0.05 is presented as "ns"; P < 0.05 is presented as "*"; P < 0.01 is presented as "**". IR1: hNECs that exposed to single irradiation; IR5: hNECs that exposed to repeated irradiation; CTRL: The untreated hNECs.

IR Modulates the Effect of Epithelium in Host Defense Against Foreign Invasion

To investigate whether the irradiation influences the antiviral and antimicrobial activity of hNECs, we treated the fully differentiated control and IR5 hNECs with Poly(I:C) and LPS, respectively, for 24 hours (Figure 6A).

25 μg/mL Poly(I:C) treatment was conducted to mimic a post-viral infection status. After 24 hours of stimulation, we observed a significant elevation of pathogen recognition receptor Toll-like receptor 3 (TLR3), antiviral type I interferon (IFNB1), type III interferon (IL-28A), and interferon-stimulated gene (RSAD2) as well as chemokine CXC ligand 10 (CXCL10) in both Poly(I:C)-treated control and Poly(I:C)-treated IR5 group in comparison to the untreated control. In addition, compared to the Poly(I:C)-treated control group, the mRNA level of TLR3 and CXCL10 increased significantly in the Poly(I:C)-treated IR5 group (Figure 6B–F).

We also treated the hNECs with 10 μg/mL LPS. After 24 hours of stimulation, the mRNA level of Toll-like receptor 4 (TLR4) and type III cytokine (IL-17A) in the LPS-treated IR5 group significantly increased compared to the untreated control. The mRNA level of IL-8 increased significantly in the LPS-treated IR5 group compared to the LPS-treated control group. No significant difference was observed in the expression of chemokine CCL2 and proinflammatory cytokine IL-6 (Figure 6G–K).

The above results suggested that repeated IR exposure modulated the epithelium host defense and leads to hyperreactive response against viral invasion.

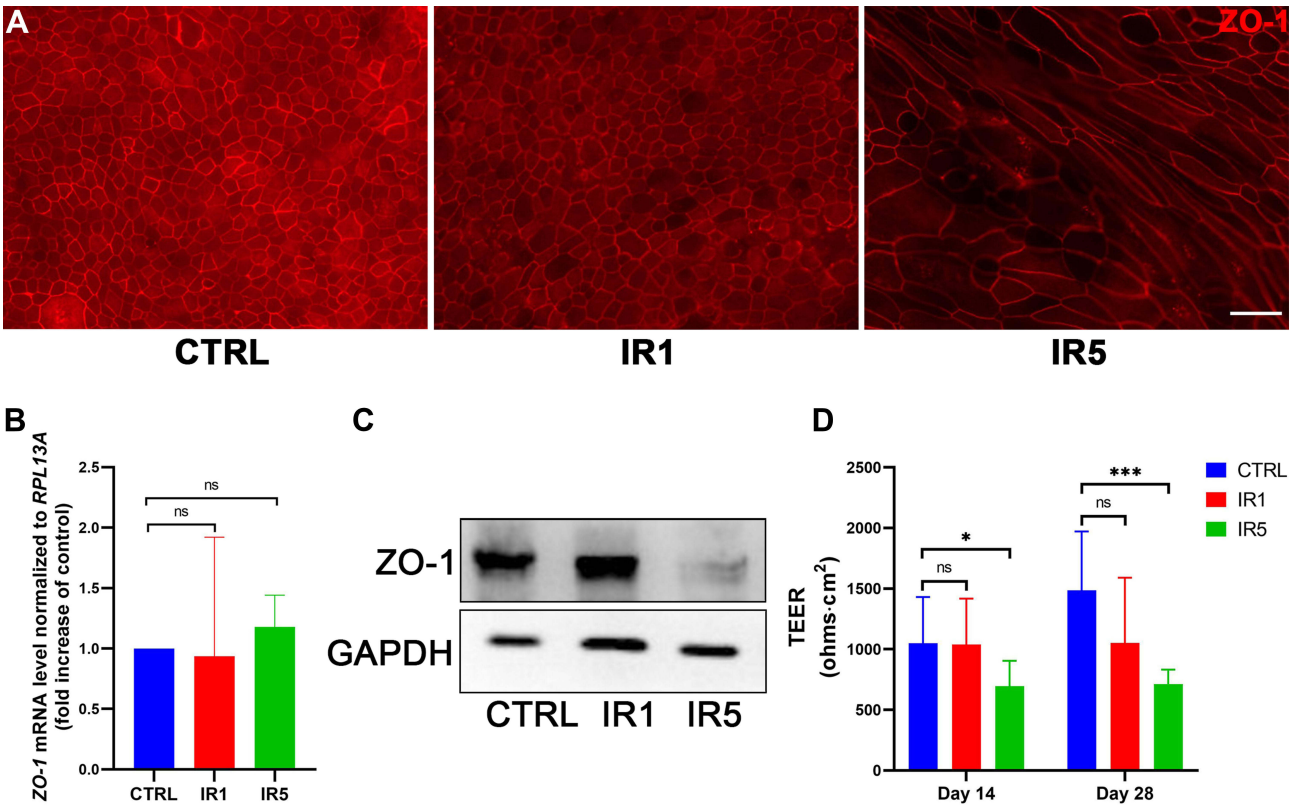

Figure 5 Effect of irradiation on epithelial integrity. (**A**) Representative transwell IF images of ZO-1 on ALI day 28 (×400 magnification, scale bar = 20 μm). (**B**) mRNA level of ZO-1 post-irradiation on ALI day 28 (n = 9). (**C**) Western blot result shows ZO-1 protein level decrease significantly post-irradiation on ALI day 28. (**D**) TEER result at ALI day 14 and 28 indicated that repeated IR exposure causes a considerable disruption of the epithelial barrier in comparison to the control, while single IR exposure did not reduce the TEER values significantly (n = 9). Error bars represent median with interquartile range. P > 0.05 is presented as "ns"; P < 0.05 is presented as "*"; P < 0.001 is presented as "***". IR1: hNECs that exposed to single irradiation; IR5: hNECs that exposed to repeated irradiation; CTRL: The untreated hNECs.

Discussion

Radiotherapy is a double-edged sword, although technique improvements have dramatically reduced the irradiation toxicity on normal tissue, there are still a number of patients suffering from associated side effects. Chronic rhinosinusitis (CRS) is one of the major treatment complications of radiotherapy in patients with NPC.[27–29] Our recent studies on IR-induced CRS show that there was a significant decreased expression level of MUC5AC and MUC5B (secretary proteins of goblet cells), α-tubulin and FOXJ1 (ciliated cells) as well as aberrant proliferation of p63+KRT5+ basal cells in NPC patients after 2–7 years of radiotherapy.[15,17] These findings indicate radiotherapy may cause long-term defects to the nasal epithelium structure. In the present study, we utilized the ALI organotypic airway tissue system to model nasal epithelial radiation injury in vitro. Our data show that IR induced DSBs appears in hNECs after IR exposure and could be repaired within 24h post-IR. We also demonstrate that repeated IR exposure reduced basal/progenitor cell proliferation, altered differentiation of ciliated cells, and inhibited mucus production, in addition to promoting mucociliary clearance dysfunction. Furthermore, IR induces loss of integrity in epithelial tight junction and compromises nasal epithelial barrier function. Finally, our data provide an evidence that repeated IR exposure increased the sensitivity of antiviral response, which resulted in epithelial host defense dysfunction.

Irradiation is known to induce DSBs and trigger DNA damage repair response in diverse mammalian organs.[30] As a common RT-related toxicity, many studies have described IR-induced DSBs' repairing kinetics in different kinds of cells.[31–33] Here, we proved that the γ-H2AX foci induced by single or repeated IR exposure followed a similar kinetics of forming and fading in hNECs. After IR exposure, the foci per nucleus increased dramatically at 1h post-IR, and almost disappeared within 24h post-IR, indicating that healthy hNECs can repair the DNA damage in a time-dependent manner. Moreover, further analysis of the number of foci >30 pixels observed a delayed foci disappearance in IR5 group at 24h post-

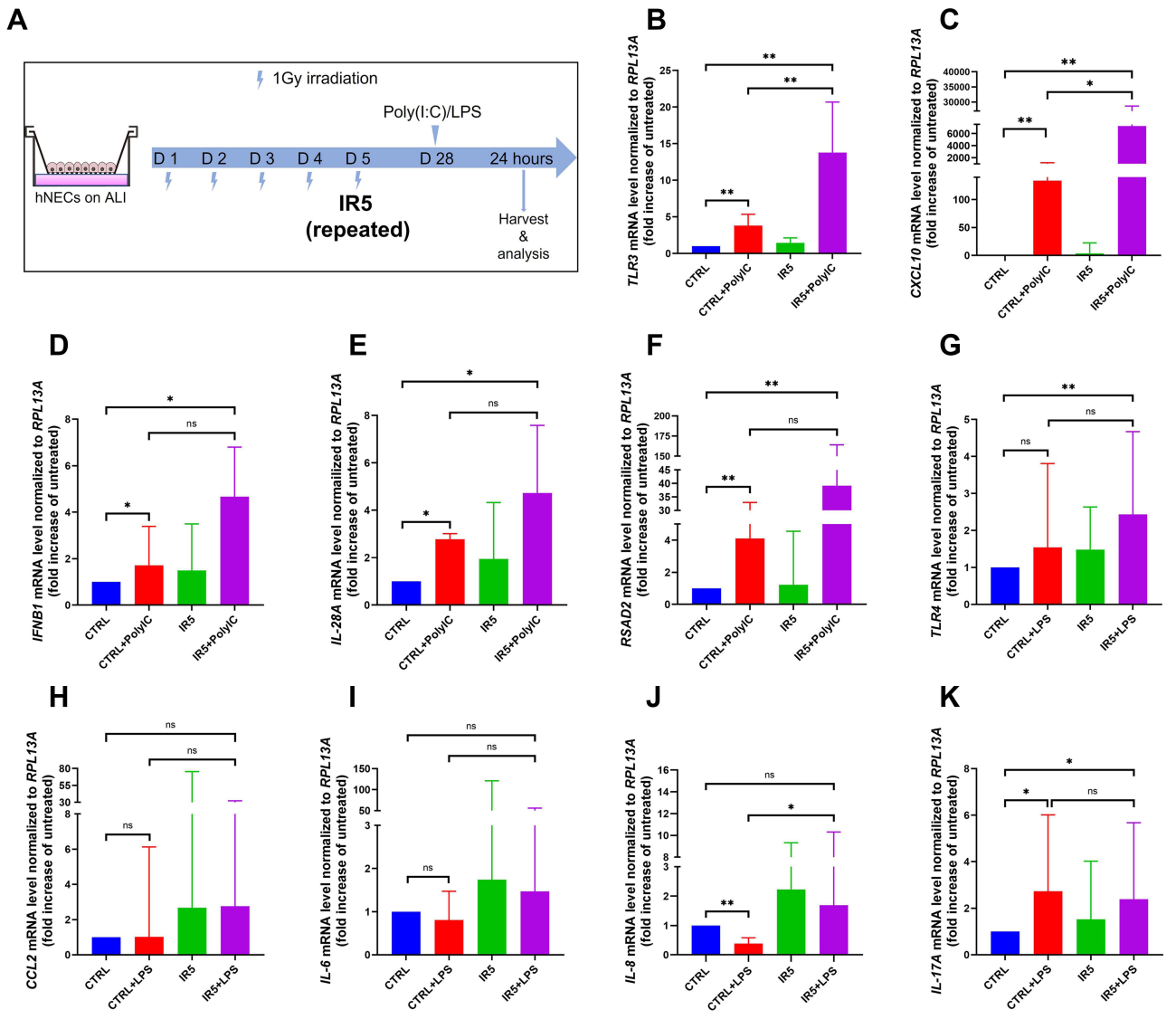

Figure 6 The mRNA level of antiviral and antimicrobial markers compared to the untreated cells (treated with 25 μg/mL Poly(I:C) or 10 μg/mL LPS, n = 6). (**A**) Schematic for stimuli treatment on matured hNECs. (**B**–**F**) TLR3, CXCL10, IFNB1, IL-28A, and RSAD2 mRNA level was increased significantly post 25 μg/mL Poly(I:C) treatment in both Poly(I:C)-treated control and Poly(I:C)-treated IR5 group in comparison to the untreated control. (**G**–**K**) TLR4 and IL-17A increased significantly post 10 μg/mL LPS treatment in the IR5 group in comparison to the untreated control. Error bars represent median with interquartile range. P > 0.05 is presented as "ns"; P < 0.05 is presented as "*"; P < 0.01 is presented as "**". IR5: hNECs that exposed to repeated irradiation; CTRL: The untreated hNECs.

IR. Persistence of unresolved foci beyond 24h post-IR suggests that repair mechanisms or efficiency have been hampered by the cumulative effect of repeated radiation. To the best of our knowledge, this is the first study to discuss the potential relationship between DNA damage repair efficiency and the size of foci in hNECs. Since the severity of nasal epithelium defects post-RT depends on the IR dose, thus, reducing peripheral doses during radiation by employing alternative radiation modalities (eg, proton beam therapy) can minimize radiation-induced side effects. Other approaches include enhancing DNA damage repair[34] or cell renewal capacity,[9,35] use of radio-protective agents or modulating inflammation.[36] The precise mechanism of DSBs' repairment requires further studies to provide insight of efficient treatment.

On the other hand, although a substantial amount of this damage may be repaired over time, we were wondering if these early events can stimulate changes in cellular function and contribute the persistent inflammation in the nasal mucosa. We next investigate the influence of IR on hNECs proliferative and differentiative ability during ALI differentiation. We observed poor proliferation dynamics with the ratio of p63/KRT5 double-positive cells and Ki67 positive cells decreased significantly in hNECs of IR5 group. Interestingly, there was no significant difference between

the IR1 and control group, which means healthy hNECs can fully repair the damage of single exposure to moderate dose IR. We also confirmed this in the differentiation stage, when our result showed that there is a dramatic reduction of ciliated and goblet cells in the IR5 group but not in the IR1 group. Furthermore, we also found that defective ciliogenesis leads to abnormal cilia ultrastructure. There was significant downregulation in the mRNA level of several motile ciliary assembly genes accompanied by decreasing CBF. Under homeostatic conditions, effective mucociliary clearance requires coordinated ciliary motility and appropriate mucus secretion. Previous studies indicated that RT damaged the mucociliary transport time,[19,37] which manifested associated clinical symptoms. Our previous study also reported that NPC patients post-RT have nasal and nasopharyngeal mucosal atrophy with decreased mucus secretion and mucosal dryness by anterior rhinoscopy.[15] The mucociliary clearance acts as the first defense mechanism for the normal respiratory system,[37,38] and our findings provided the evidence that IR-induced cellular dysfunction of goblet cells and ciliated cells might be responsible for the long-term or recurrent nasal or paranasal symptoms in patients post-RT. Taken together, IR disrupts the basal cell's self-renewal potential which then results in impairing the hNECs differentiative ability to form epithelium fully. This vicious cycle of IR-induced damage and aberrant repair process of nasal epithelial cells may lead to progressive nasal epithelium damage and impair its function.

Another important function of nasal epithelium is its physical barrier against the external environment. Early disruption of cell–cell tight junctions may lead to foreign substances invasion and indeed further trigger mucosal inflammation. Several studies have described the negative effect of irradiation on the respiratory[9] and intestinal[7] epithelial barrier, featured by tight junction defects. In this study, we found an irregular staining pattern of typical TJ protein ZO-1 together with reduced protein expression. Moreover, we observed a significant drop of TEER value in the IR5 group on both ALI day 14 and day 28. Our findings suggest that the repeated IR exposure at the initial stage, the irradiated hNECs might not be competent for forming functional barrier. However, in a recent study by O'Sullivan et al, they have reported that moderate dose (1Gy) irradiation provoked unjamming transition in primary human bronchial (HBE) cells but disrupted neither normal differentiation nor the integrity of the epithelial cell layer.[39] The discordant result is likely due to the different experiment setups. In their study, HBE cells were exposed to radiation on Day 7,10 and 14 of ALI culture. However, we performed a five consecutive days exposure from the moment of ALI introduction (ALI day 0) which is closely mimic the clinical radiotherapy on NPC as previously stated. Besides, a couple of studies also show that the proliferation of basal progenitor cell dominant at the first two days of ALI culture while the genes related to the process of cilia and goblet cell differentiation started expression within the first 3–7 days of ALI culture and gradually increased until terminally differentiated.[40–42] Therefore, our model better elucidate the molecular events that underline changes in the proliferation and differentiation of nasal epithelial cell induced by moderate dose radiation exposure.

Since IR has a direct effect on the hNECs, the structural and functional changes of the nasal epithelium may lead to reduce the ability of resist infection and host innate immune system. TLRs are one of the most important pattern recognition receptors (PRRs) and play a crucial role in initiating innate immune response.[43] Previous study suggests that IR can induce the activation of innate immune response through TLR-dependent pathway and exaggerate the adaptive immune response.[44] Inflammation is considered as a protective immune response against foreign invaders; however, hyper-inflammation always leads to tissue damage.[45] Our pathogen stimulating experiments revealed a hyperactive response to viral [Poly(I:C)] or bacterial (LPS) surrogates in irradiated cells, especially the significant increase of the pathogen entry receptors TLR3 and TLR4 on epithelial cells. The expression of TLRs would potentially increase susceptibility to particular infections. In addition, we found that TLRs activation induces the secretion of type I and III interferons, such as IFNB1 and IL-28A here which also can activate expression of proinflammatory cytokines (IL-6, IL-8 and IL-17A) and chemokines (CCL2 and CXCL10). Ultimately, the overactivation of these mediators leads to disruption of immune homeostasis and contribute the development of the pathological process such as chronic airway inflammation. Therefore, management of the inflammatory effectors after exposure to IR may help to reduce the risk of these diseases among individuals to RT.

Our study still has certain limitations. First and foremost, we scored the γ-H2AX foci manually, which might be inaccurate and biased. Because of the limited resolution of our immunofluorescent microscope and the saturation effect (reaching a maximum level of detectable foci due to physical/imaging foci overlapping),[5] we can hardly distinguish whether bigger foci are overlapping foci or a single focus. According to Tanja Bulat's study, foci was detected using

Cellprofiler software, which automatically picks out foci within 6–30 pixels but did not include the foci over 30 pixels.[46] Thus, a high-resolution or confocal microscope could help to capture a more precise image, and proper counting strategies can provide more credible scores of γ-H2AX foci.[47] Irradiation has more than one way to induce DNA damage. In our study, we focused on detecting DNA DSB since DSBs are considered the most lethal type of DNA damage. However, IR induces multiple types of damage to the DNA, as well as to other biomolecules, which are likely to further impair cell function and might account for some of our observations.[48] Last but not least, we cannot ignore the paradoxical results between the mRNA and protein level. There is research demonstrating that DNA damage suppresses the ribosomal DNA transcription and may potentially inhibit the protein translation.[49] Clarifying these mechanisms needs further explorations.

Conclusion

Our study demonstrates that, even at moderate amounts of radiation akin to peripheral doses hNECs exhibit reduced proliferation and differentiation capability with barrier dysfunction in response to repeated IR exposure. These findings suggest that the pathophysiologic mechanism of chronic and recurrent upper respiratory tract infection and inflammation (eg, chronic rhinosinusitis) in NPC patients after radiotherapy could be attributed to IR-induced prolonged structural and functional impairments of hNECs. This knowledge deepens our understanding of the extend of normal tissue damage of irradiation and helps in improving precision to minimize radiotherapy-induced toxicities.

Institutional Review Board Statement

The study was conducted in accordance with the Declaration of Helsinki and approved by the institutional review boards of the National Healthcare Group Domain Specific Review Board of Singapore (DSRB D/11/228 and IRB 13–509).

Data Sharing Statement

The data presented in this study are available on request from the corresponding author.

Informed Consent Statement

All participants gave informed consent to participate in the study.

Acknowledgment

The authors wish to thank Tze-yen Chua and Lakshmi Jayakumar for their excellent technical assistance, and the Department of Physics, National University of Singapore, for use of the gamma irradiator. We also want to express our gratitude to Dr Jennie Wong and Dr Rupangi Verma, Medical and Scientific Communication, Research Support Unit, Yong Loo Lin School of Medicine, National University Health System, for assistance in the language editing of this manuscript.

Author Contributions

All authors made a significant contribution to this study, whether that is in the conception, study design, execution, acquisition of data, analysis, and interpretation, or in all these areas. All authors contributed to data analysis, drafting, revising, or critically reviewing the article, have agreed on the journal to which the article will be submitted, gave final approval of the version to be published, and agree to be accountable for all aspects of the work.

Funding

This research was funded by the National Medical Research Council, Singapore No. NMRC/CIRG/1458/2016 (to De-Yun Wang), and National Natural Science Foundation of China No. 81873690 & No. 82171104 (to Qian-Hui Qiu).

Disclosure

The authors report no conflicts of interest in this work.

References

1. Gong L, Zhang Y, Liu C, Zhang M, Han S. Application of radiosensitizers in cancer radiotherapy. *Int J Nanomedicine*. 2021;16:1083–1102. doi:10.2147/IJN.S290438
2. Kuo LJ, Yang L-X. Gamma-H2AX - a novel biomarker for DNA double-strand breaks. *In Vivo*. 2008;22(3):305–309.
3. Paull TT, Rogakou EP, Yamazaki V, Kirchgessner CU, Gellert M, Bonner WM. A critical role for histone H2AX in recruitment of repair factors to nuclear foci after DNA damage. *Curr Biol*. 2000;10(15):886–895. doi:10.1016/S0960-9822(00)00610-2
4. Ricoul M, Gnana Sekaran TS, Brochard P, Herate C, Sabatier L. γ-H2AX foci persistence at chromosome break suggests slow and faithful repair phases restoring chromosome integrity. *Cancers*. 2019;11(9):1397. doi:10.3390/cancers11091397
5. Mariotti LG, Pirovano G, Savage KI, et al. Use of the γ-H2AX assay to investigate DNA repair dynamics following multiple radiation exposures. *PLoS One*. 2013;8(11):e79541. doi:10.1371/journal.pone.0079541
6. Bonner WM, Redon CE, Dickey JS, et al. GammaH2AX and cancer. *Nat Rev Cancer*. 2008;8(12):957–967. doi:10.1038/nrc2523
7. Kwak SY, Jang WI, Park S, et al. Metallothionein 2 activation by pravastatin reinforces epithelial integrity and ameliorates radiation-induced enteropathy. *EBioMedicine*. 2021;73:103641. doi:10.1016/j.ebiom.2021.103641
8. Yang C, Tang H, Wang L, et al. Dimethyl sulfoxide prevents radiation-induced oral mucositis through facilitating DNA double-strand break repair in epithelial stem cells. *Int J Radiat Oncol Biol Phys*. 2018;102(5):1577–1589. doi:10.1016/j.ijrobp.2018.07.2010
9. Giuranno L, Roig EM, Wansleeben C, et al. NOTCH inhibition promotes bronchial stem cell renewal and epithelial barrier integrity after irradiation. *Stem Cells Transl Med*. 2020;9(7):799–812. doi:10.1002/sctm.19-0278
10. Chan ATC. Nasopharyngeal carcinoma. *Ann Oncol*. 2010;21(Suppl 7):vii308–vii312. doi:10.1093/annonc/mdq277
11. Chen Y-P, Chan ATC, Le Q-T, Blanchard P, Sun Y, Ma J. Nasopharyngeal carcinoma. *Lancet*. 2019;394(10192):64–80. doi:10.1016/S0140-6736(19)30956-0
12. Bossi P, Chan AT, Licitra L, et al. Nasopharyngeal carcinoma: ESMO-EURACAN clinical practice guidelines for diagnosis, treatment and follow-up. *Ann Oncol*. 2021;32(4):452–465. doi:10.1016/j.annonc.2020.12.007
13. Lee AWM, Sze WM, Au JSK, et al. Treatment results for nasopharyngeal carcinoma in the modern era: the Hong Kong experience. *Int J Radiat Oncol Biol Phys*. 2005;61(4):1107–1116. doi:10.1016/j.ijrobp.2004.07.702
14. Teo PML, Ma BBY, Chan ATC. Radiotherapy for nasopharyngeal carcinoma–transition from two-dimensional to three-dimensional methods. *Radiother Oncol*. 2004;73(2):163–172. doi:10.1016/j.radonc.2004.06.005
15. Zhou S, Huang H, Chen Q, et al. Long-term defects of nasal epithelium barrier functions in patients with nasopharyngeal carcinoma post chemo-radiotherapy. *Radiother Oncol*. 2020;148:116–125. doi:10.1016/j.radonc.2020.03.038
16. Su Y-X, Liu L-P, Li L, et al. Factors influencing the incidence of sinusitis in nasopharyngeal carcinoma patients after intensity-modulated radiation therapy. *Eur Arch Otorhinolaryngol*. 2014;271(12):3195–3201. doi:10.1007/s00405-014-3004-8
17. Huang H, Tan KS, Zhou S, et al. p63Krt5 basal cells are increased in the squamous metaplastic epithelium of patients with radiation-induced chronic Rhinosinusitis. *Radiat Oncol*. 2020;15(1):222. doi:10.1186/s13014-020-01656-7
18. Stringer SP, Stiles W, Slattery WH, et al. Nasal mucociliary clearance after radiation therapy. *Laryngoscope*. 1995;105(4 Pt 1):380–382. doi:10.1288/00005537-199504000-00008
19. Gurushekar PR, Isiah R, John S, Sebastian T, Varghese L. Effects of radiotherapy on olfaction and nasal function in head and neck cancer patients. *Am J Otolaryngol*. 2020;41(4):102537. doi:10.1016/j.amjoto.2020.102537
20. Deprez M, Zaragosi L-E, Truchi M, et al. A single-cell atlas of the human healthy airways. *Am J Respir Crit Care Med*. 2020;202(12):1636–1645. doi:10.1164/rccm.201911-2199OC
21. Li CW, Shi L, Zhang KK, et al. Role of p63/p73 in epithelial remodeling and their response to steroid treatment in nasal polyposis. *J Allergy Clin Immunol*. 2011;127(3):765–772.e2. doi:10.1016/j.jaci.2010.12.011
22. Fukuoka A, Yoshimoto T. Barrier dysfunction in the nasal allergy. *Allergol Int*. 2018;67(1):18–23. doi:10.1016/j.alit.2017.10.006
23. Amatngalim GD, Schrumpf JA, Dishchekenian F, et al. Aberrant epithelial differentiation by cigarette smoke dysregulates respiratory host defence. *Eur Respir J*. 2018;51(4):1701009. doi:10.1183/13993003.01009-2017
24. Li YY, Li CW, Chao SS, et al. Impairment of cilia architecture and ciliogenesis in hyperplastic nasal epithelium from nasal polyps. *J Allergy Clin Immunol*. 2014;134(6):1282–1292. doi:10.1016/j.jaci.2014.07.038
25. Zhao X, Yu F, Li C, et al. The use of nasal epithelial stem/progenitor cells to produce functioning ciliated cells in vitro. *Am J Rhinol Allergy*. 2012;26(5):345–350. doi:10.2500/ajra.2012.26.3794
26. Chen Q, Tan KS, Liu J, et al. Host antiviral response suppresses ciliogenesis and motile ciliary functions in the nasal epithelium. *Front Cell Dev Biol*. 2020;8:581340. doi:10.3389/fcell.2020.581340
27. Dilalla V, Chaput G, Williams T, Sultanem K. Radiotherapy side effects: integrating a survivorship clinical lens to better serve patients. *Curr Oncol*. 2020;27(2):107–112. doi:10.3747/co.27.6233
28. Wu P-W, Huang -C-C, Lee Y-S, et al. Post-irradiation sinus mucosa disease in nasopharyngeal carcinoma patients treated with intensity-modulated proton therapy. *Cancers*. 2022;14(1):225. doi:10.3390/cancers14010225
29. Lu Y-T, Lu Y-C, Cheng H-C, et al. Chronic rhinosinusitis after radiotherapy in patients with head and neck cancer: a population-based cohort study in Taiwan. *Int Forum Allergy Rhinol*. 2020;10(5):692–697. doi:10.1002/alr.22526
30. Miyake T, Shimada M, Matsumoto Y, Okino A. DNA damage response after ionizing radiation exposure in skin keratinocytes derived from human-induced pluripotent stem cells. *Int J Radiat Oncol Biol Phys*. 2019;105(1):193–205. doi:10.1016/j.ijrobp.2019.05.006
31. Brand M, Ellmann S, Sommer M, et al. Influence of cardiac MR imaging on DNA double-strand breaks in human blood lymphocytes. *Radiology*. 2015;277(2):406–412. doi:10.1148/radiol.2015150555
32. Eleuteri B, Aranda S, Ernfors P. NoRC recruitment by H2A.X deposition at rRNA gene promoter limits embryonic stem cell proliferation. *Cell Rep*. 2018;23(6):1853–1866. doi:10.1016/j.celrep.2018.04.023
33. Frame FM, Savoie H, Bryden F, et al. Mechanisms of growth inhibition of primary prostate epithelial cells following gamma irradiation or photodynamic therapy include senescence, necrosis, and autophagy, but not apoptosis. *Cancer Med*. 2016;5(1):61–73. doi:10.1002/cam4.553
34. Kitabatake K, Kaji T, Tsukimoto M. ATP and ADP enhance DNA damage repair in γ-irradiated BEAS-2B human bronchial epithelial cells through activation of P2X7 and P2Y12 receptors. *Toxicol Appl Pharmacol*. 2020;407:115240. doi:10.1016/j.taap.2020.115240

35. Cho J, Bing SJ, Kim A, et al. Beetroot (Beta vulgaris) rescues mice from γ-ray irradiation by accelerating hematopoiesis and curtailing immunosuppression. *Pharm Biol*. 2017;55(1):306–319. doi:10.1080/13880209.2016.1237976
36. Wang H, Ahn KS, Alharbi SA, et al. Celastrol alleviates gamma irradiation-induced damage by modulating diverse inflammatory mediators. *Int J Mol Sci*. 2020;21(3). doi:10.3390/ijms21031084
37. Kılıç C, Tunçel Ü, Cömert E, Kaya BV. The effect of radiotherapy on mucociliary clearance in patients with laryngeal and nasopharyngeal cancer. *Eur Arch Otorhinolaryngol*. 2015;272(6):1517–1520. doi:10.1007/s00405-014-3082-7
38. Bustamante-Marin XM, Ostrowski LE. Cilia and mucociliary clearance. *Cold Spring Harb Perspect Biol*. 2017;9(4):a028241. doi:10.1101/cshperspect.a028241
39. O'Sullivan MJ, Mitchel JA, Das A, et al. Irradiation induces epithelial cell unjamming. *Front Cell Dev Biol*. 2020;8:21. doi:10.3389/fcell.2020.00021
40. Gras D, Petit A, Charriot J, et al. Epithelial ciliated beating cells essential for ex vivo ALI culture growth. *BMC Pulm Med*. 2017;17(1):80. doi:10.1186/s12890-017-0423-5
41. Yuan T, Zheng R, Liu J, et al. Role of yes-associated protein in interleukin-13 induced nasal remodeling of chronic rhinosinusitis with nasal polyps. *Allergy*. 2021;76(2):600–604. doi:10.1111/all.14699
42. Bukowy-Bieryłło Z, Daca-Roszak P, Jurczak J, et al. In vitro differentiation of ciliated cells in ALI-cultured human airway epithelium - The framework for functional studies on airway differentiation in ciliopathies. *Eur J Cell Biol*. 2022;101(1):151189. doi:10.1016/j.ejcb.2021.151189
43. Mohammad NS, Nazli R, Zafar H, Fatima S. Effects of lipid based Multiple Micronutrients Supplement on the birth outcome of underweight pre-eclamptic women: a randomized clinical trial. *Pak J Med Sci*. 2022;38(1):219–226. doi:10.12669/pjms.38.1.4396
44. Roses RE, Xu M, Koski GK, Czerniecki BJ. Radiation therapy and Toll-like receptor signaling: implications for the treatment of cancer. *Oncogene*. 2008;27(2):200–207. doi:10.1038/sj.onc.1210909
45. Bennett JM, Reeves G, Billman GE, Sturmberg JP. Inflammation-nature's way to efficiently respond to all types of challenges: implications for understanding and managing "the epidemic" of chronic diseases. *Front Med*. 2018;5:316. doi:10.3389/fmed.2018.00316
46. Bulat T, Keta O, Korićanac L, et al. Radiation dose determines the method for quantification of DNA double strand breaks. *An Acad Bras Cienc*. 2016;88(1):127–136. doi:10.1590/0001-3765201620140553
47. Kinner A, Wu W, Staudt C, Iliakis G. Gamma-H2AX in recognition and signaling of DNA double-strand breaks in the context of chromatin. *Nucleic Acids Res*. 2008;36(17):5678–5694. doi:10.1093/nar/gkn550
48. Kavanagh JN, Redmond KM, Schettino G, Prise KM. DNA double strand break repair: a radiation perspective. *Antioxid Redox Signal*. 2013;18(18):2458–2472. doi:10.1089/ars.2012.5151
49. Dong C, An L, Yu C-H, Huen MSY. A DYRK1B-dependent pathway suppresses rDNA transcription in response to DNA damage. *Nucleic Acids Res*. 2021;49(3):1485–1496. doi:10.1093/nar/gkaa1290